# List of Supplemental Material

Figure S1. Temperature advection associated with AD (shaded, K day-1) shown with the wind at 500 hPa (vector, m/s) for (a) the early (1982-1997) and (b) the recent (1998-2013) period. Temperature advection is calculated by $\hat{V}'\cdot\nabla\bar{T} + \bar{V}\cdot\nabla\hat{T}' + V'\cdot\nabla\hat{T}'$, where $\bar{V}$ and $\bar{T}$ are time-mean 500 hPa wind and air temperature in each period, respectively, and. V' and T' are regressed wind and air temperature onto the AD index, respectively.

Figure S2. Regression patterns of outgoing long-radiation (OLR, W $m^{-2}$) onto the AD index for (a) the early (1982-1997) and (b) the recent (1998-2013) period. OLR data is obtain from NOAA [Liebmann and Smith, 1996]. The AD index was reversed in sign for the melting phase of sea ice. Dotted area indicates the statistically significant region at 95% confidence level.

Figure S3. Leading EOF modes for the negative PDO phase before 1998. (a) is EOF1 and (b) is EOF2.

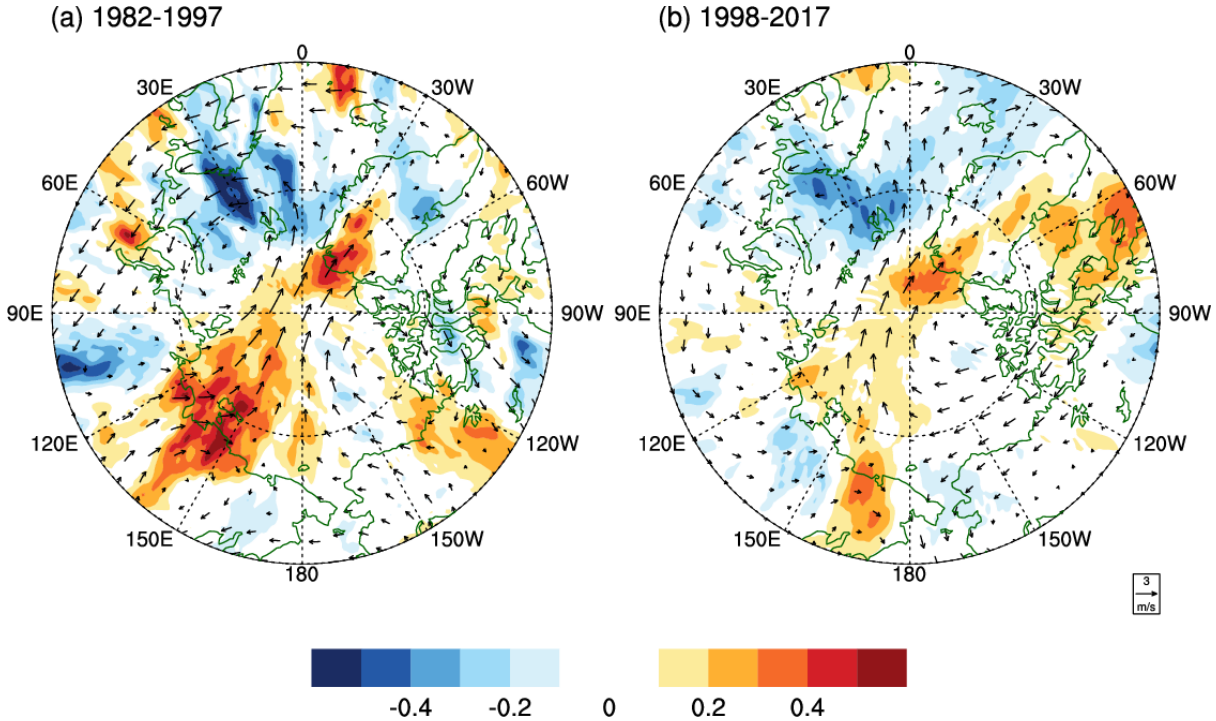


Figure S1. Temperature advection associated with AD (shaded, K day-1) shown with the wind at 500 hPa (vector, m/s) for (a) the early (1982-1997) and (b) the recent (1998-2013) period. Temperature advection is calculated by $\hat{V}'\cdot\nabla\bar{T}+\bar{V}\cdot\nabla\hat{T}'+V'\cdot\nabla\hat{T}'$, where $\bar{V}$ and $\bar{T}$ are time-mean 500 hPa wind and air temperature in each period, respectively, and. V' and T' are regressed wind and air temperature onto the AD index, respectively.

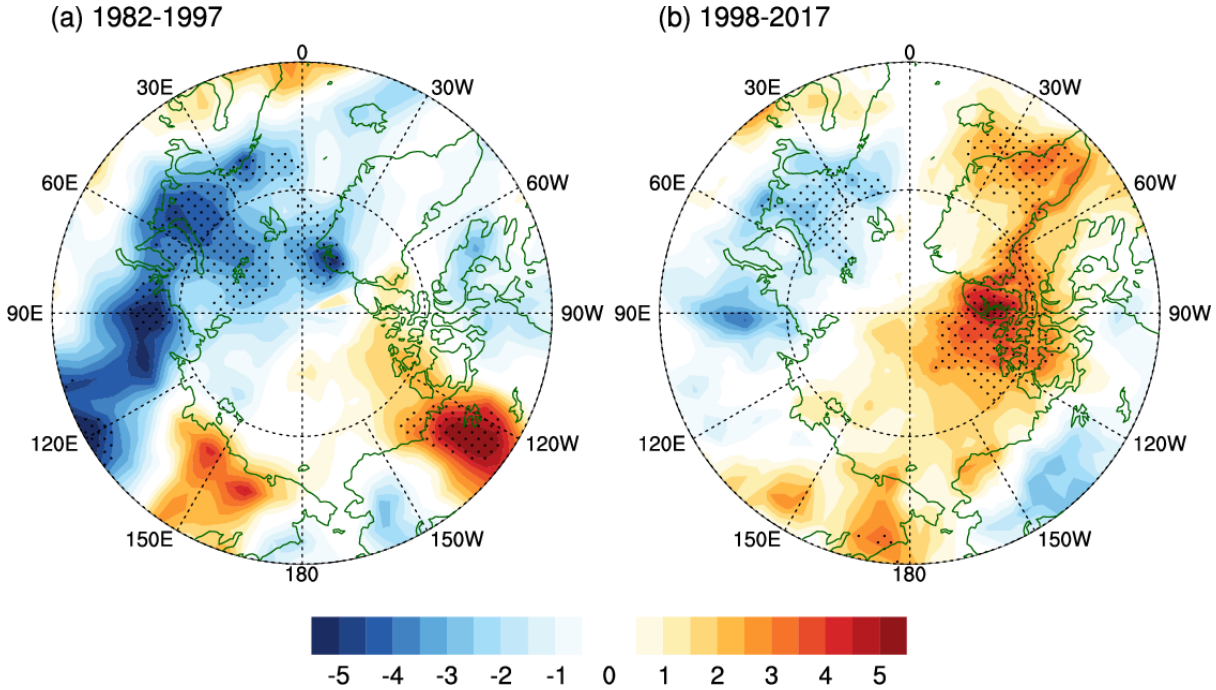


Figure S2. Regression patterns of outgoing long-radiation (OLR, W $m^{-2}$) onto the AD index for (a) the early (1982-1997) and (b) the recent (1998-2017) period. OLR data is obtain from NOAA [Liebmann and Smith, 1996]. The AD index was reversed in sign for the melting phase of sea ice. Dotted area indicates the statistically significant region at 95% confidence level.

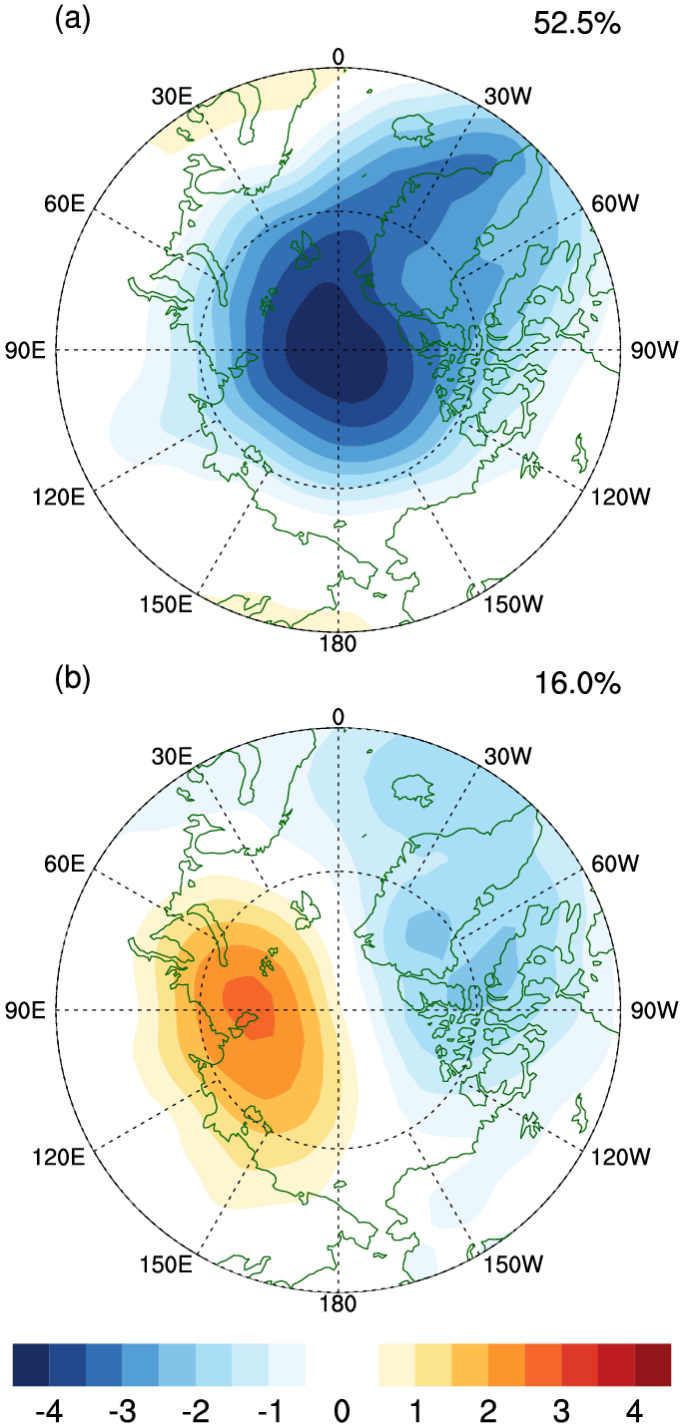


Figure S3. Leading EOF modes for the negative PDO phase before 1998. (a) is EOF1 and (b) is EOF2.